18èmes Journées Internationales de Thermique (JITH 2017)
Monastir (Tunisie), 25 - 27 Octobre 2017

Numerical Investigation of Heat Pipe Behavior Using OpenFOAM Software

Authors: **AROUA GHEDIRA, ZIED LATAOUI, ABDELMAJID JEMNI**

Adress of the authors: Laboratory of Thermal and Energetic Systems Studies (LESTE) at the National School of Engineering of Monastir, University of Monastir, Tunisia.

Emails of the authors: ***rourough@yahoo.fr;*** *zied_lataoui@yahoo.fr;* *abdelmajid.jemni@enim.rnu.tn*

Abstract: Heat pipes are efficient heat transfer devices based on evaporation-condensation phenomenon. They used the latent heat of vaporization to transport heat, even for a small temperature difference. Due to their great performance, their use has become increasingly common in some terrestrial and spatial applications and they continue to interest researchers. Heat pipes with capillary structure and particularly wick structure, arouses our interest.

The objective of the current investigation is to develop a model using the open-source software OpenFOAM to simulate the behavior of heat pipe with capillary wick structure. We are focusing in this study in simulating the phase change liquid-vapor phenomena using “OpenFOAM”. The variations of the axial temperature in the wick and vapor core are studying with different heat applied at the evaporator.

Keywords: heat pipe, OpenFOAM, phase change

1. Introduction

Since the invention of the heat pipe by Grover et al. (1964), there has been renewed interest in the use of heat pipes for thermal management due to increasing heat flux requirements and thermal constraints in many industrial applications. Many investigations have been performed concerning heat pipe operating limits, heat pipe applications, and design modifications to improve heat pipe performance. The performance of heat pipes is characterized both by its overall effective thermal resistance and its maximum power in horizontal and vertical positions. These characteristics depend mainly on the capillary structure which is usually made of grooves, meshes, sintered powder or a combination of them [1].

Heat pipes are, in many applications, circular and are used to transport heat from one heat source to one heat sink. Also, there are flat heat pipes which have the same components, but offer a wide cross-section, and this allows reducing their thickness without reducing their thermal performance.

A heat pipe has the advantage over other conventional methods that it can transport heat over a considerable distance with no additional power input to the system [2]. It can also be used in a solar water heater [3] or solar cooker [4].

There have been some direct measurements in the vapor core of wicked heat pipes under steady state operation. El-Genk and Huang [5] measured the vapor temperature distribution of a copper-water heat pipe during transient operation, but presented data for only a single steady-state case. Kempers et al. [6] investigated the effect of various operating conditions on the thermal resistances of the evaporator and the condenser of a wicked heat pipes.

The volume-of-fluid (VOF) approach is a mature technique for simulating two-phase flows but the phase-change simulation is still in its infancy. Liquid-vapor phase change plays a key role in many energy-intensive processes. The objective of the current investigation is to develop a model using the open-source environment OpenFOAM for liquid-vapor phase change.

OpenFOAM (Open Source Field Operation and Manipulation) is an open source software package written in C++ for the solution of Continuum Mechanics problems based on Finite Volume Method (FVM), in particularly CFD. Its initial development can be dated back to late 1980s at Imperial College, London.

Multiple expressions for phase change have been proposed in the literature but few implementations are publicly available with OpenFoam. Martin Andersen [7] used interphaseChangeFoam and implemented transport temperature dependent phase change algorithm. Here, we are adapting this solver to take into accounts Darcy term and Clausius-Clapeyron equation to study the effect of the variation of heat input applied to the evaporator in the temperature of the wick and the vapor core.

2. Description of the problem

The heat pipe is divided in three radial regions: wall, wick and vapor core. It is also divided in three axial sections: evaporator section, adiabatic section, and condenser section.

The wick is saturated with liquid phase of the working fluid to prevent dryout, and the remaining volume of the tube contains the vapor phase. Heat applied at the evaporator section causes the liquid to vaporize into the vapor space. The vapor flows to the condenser and releases latent heat as it condenses. The released heat is ejected into the environment from the outer condenser surface as shown schematically in Figure. 1.

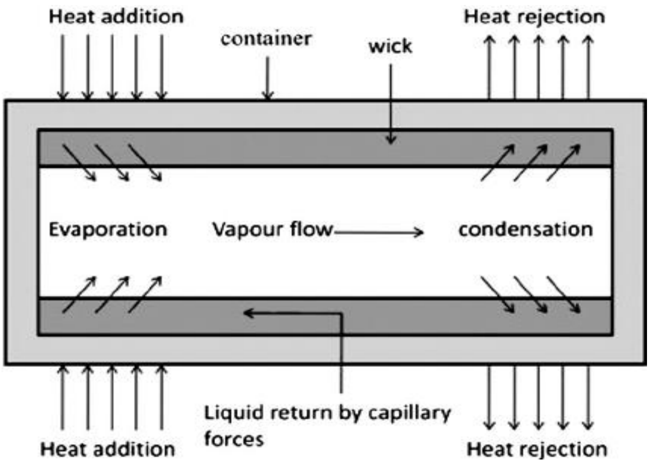

Figure 1: Schematic of the heat pipe

To simplify the problem, we will focus here in the phase change phenomena between the wick and vapor core. We will implement different equations of these two regions in OpenFoam's solver.

3. Mathematical model

2.1 Governing equations

In present study, two-dimensional analysis includes the liquid wick and the vapor core of the heat pipe. The governing equations may be written as shown below, following the development in [8].
The continuity equation for the wick and the vapor core is:

$$\varepsilon \frac{\partial \rho}{\partial t} + \nabla.(\rho U) = 0 \qquad (1)$$

The momentum equation for the wick and the vapor core is:

$$\frac{\partial(\rho U)}{\partial t} + \nabla(\rho \vec{U}\vec{U}) = -\nabla(\varepsilon p) + \nabla(\mu \nabla U) - \frac{\mu\varepsilon}{k} U \qquad (2)$$

In the vapor, permeability k= ∞ and porosity ε =1.
The energy equation in the wick and the vapor core is:

$$\frac{\partial(\rho C_p)_m T}{\partial t} + \nabla((\rho C_p)_m U T) = \nabla(K_{eff} \nabla T) \qquad (3)$$

Here $(\rho C_p)_m$ assumes different values:

For the wick: $(\rho C_p)_m = (1-\varepsilon)(\rho C_p)_{wick} + \varepsilon(\rho C_p)_l$

For the vapor core: $(\rho C_p)_m = (\rho C_p)_v$

Also, K_{eff} is the effective conductivity in the region of interest (wick or vapor).

2.2 Boundary Conditions:

- wick-wall and vapor-wall interface: $u = v = 0$
- For the outer pipe wall surface:

Evaporator

$$K_{wall} \left.\frac{\partial T}{\partial r}\right|_{r=R_0} = Q \qquad (4)$$

Adiabatic

$$\left.\frac{\partial T}{\partial r}\right|_{r=R_0} = 0 \qquad (5)$$

Condenser (convection)

$$-K_{wall} \left.\frac{\partial T}{\partial r}\right|_{r=R_0} = h\left(T_{wall} - T_a\right) \qquad (6)$$

Where h is the convective heat transfer coefficient, T_{wall} and T_a, are the outer wall surface temperature and the environment temperature, respectively.

- lateral walls : $u = v = 0$ and $\frac{\partial T}{\partial x} = 0$ (7)
- wick-vapor interface

Phase of change from liquid to vapor is assumed to occur at the wick-vapor core interface.
The interface temperature Ti is obtained from the energy balance at the interface:

$$-k_w A_i \frac{\partial T}{\partial y} + m_i C_{p_l} T_i = -k_v A_i \frac{\partial T}{\partial y} + m_i C_{p_v} T_i = m_i h_{fg} \qquad (8)$$

Here m_i<0 denotes evaporation, and m_i >0 denotes condensation.
The interface pressure Pi is obtained from Clausius-Clapeyron equation, with P_0 and T_0 being reference values:

$$\frac{R}{h_{fg}} \ln\left(\frac{P_i}{P_0}\right) = \frac{1}{T_0} - \frac{1}{T_i} \qquad (9)$$

2.3. Numerical Procedure

The equations, given in section 2.1, were implemented by modifying an existing OpenFOAM solver, interPhaseChangeFoam which is a solver for 2 incompressible, isothermal immiscible fluids with phase change. It uses a VOF (volume of fluid) phase fraction based interface capturing approach but it does include energy equation.

So we implement the energy equation for the wick and vapor core considering Darcy term in the wick. The temperature is depending on phase change (Clausius Clapeyron equation).

Three different phase change models are provided with the interPhaseChangeFoamv solver.

Here the Merkle mass transfer model is used with the mass transfer for vaporization and condensation are respectively [9]:

$$m^- = \frac{C_v \rho_v}{\frac{1}{2}\rho_l U_\infty^2 t_\infty} \alpha \min(0, p - p_{sat}) \qquad (10)$$

$$m^+ = \frac{C_c}{\frac{1}{2} U_\infty^2 t_\infty} (1-\alpha) \max(0, p - p_{sat}) \qquad (11)$$

Where $C_c, C_v, t_\infty, U_\infty$ are empirical constants based on the mean flow.

4. Results and Discussion

4.1. Validation of phase change model

The one dimensional Stefan problem was introduced for solidification at first [10] but it became a well-known benchmark for boiling simulation [11]. However, it can be conducted as a validation case for any one dimensional phase change phenomena.

In this step, Stefan problem is used to validate our solver and here the condensation phenomena. The schematic of Stefan problem is illustrated in figure2.

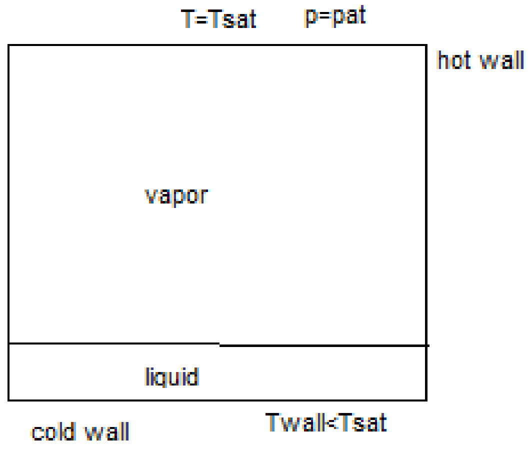

Figure 2: Schematic of Stefan problem

Heat is transferred by conduction from saturated vapor phase to liquid phase and it is rejected through subcooled wall. The vapor phase condensation leads to a motion of the interface to the top. The liquid vapor thermo physical properties for water at saturation pressure 0.130 MPa is chosen and displayed in table 1.

Table 1. Thermophysical properties of water at saturation temperature (T_{sat}=380.26K, P_{sat}=0.13 MPa)

Description	Liquid	Vapor
Density	9953.13 *kg/m*^{3}	0.75453 *kg/m*^{3}
Viscosity	2.6E-04 *Pa.s*	1.25E-05 *Pa.s*
Thermal conductivity	0.681 *w/m K*	0.0259 *w/m K*
Specific heat	4.224 *kJ/kg.K*	2.11 *kJ/kg.K*
Latent heat	2237.41 *kJ/kg*	

The analytical solution of this problem is given as [12]:

$$x(t) = 2\eta\sqrt{d_l t} \tag{12}$$

Where x is the interface position from cold wall, d_l is the liquid thermal diffusivity and η is determined from:

$$\eta \exp(\eta^2) \operatorname{erf}(\eta) = \frac{c_{p_l}(T_{sat} - T_{wall})}{\sqrt{\pi} h_{fg}} \tag{13}$$

erf is the error function.

A quasi 1D computational domain with only one grid cell in the direction of translational invariance is considered. In order to ensure that the coefficient of mass flux in energy equation is constant in CFD model during phase change process, liquid and vapor phases specific heat are assumed equal (C_{pG}=C_{pL}(P_{sat})). No slip boundary condition is employed for velocity boundary condition at the walls. Temperature of cold wall is 10 less than saturation temperature.

Result of the comparison between exact solution and CFD model for Stefan problem is depicted in figure3.

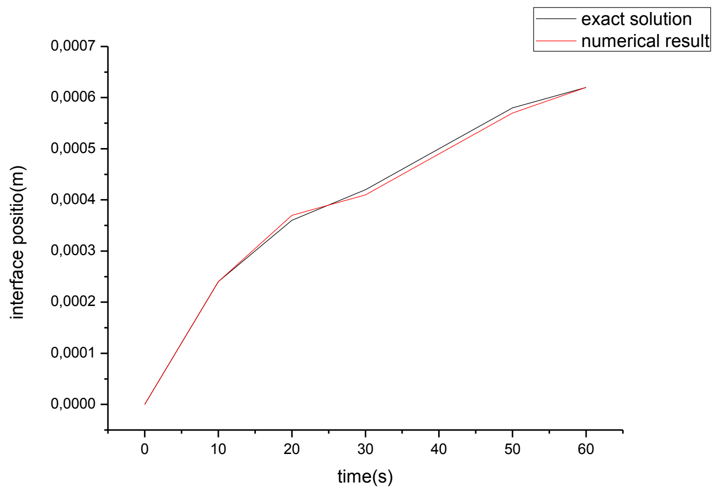

Figure 3: comparison between exact solution and CFD model for Stefan problem

There is an excellent agreement between present numerical result and exact solution.

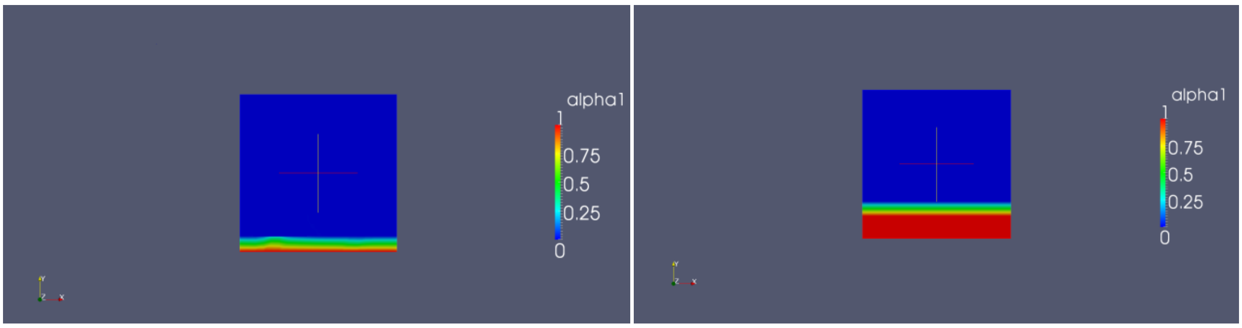

Figure 4: CFD model for Stefan problem

CFD result for Stefan problem is shown in figure 4. We can see the movement of the interface. Here, alpha = 1 represent the liquid phase, alpha =0 is the vapor phase and alpha between [0, 1] is the interface.

4.1. Heat pipe model

4.2.1. Heat pipe data

The heat pipe studying in this section is as shown schematically in Figure 5.

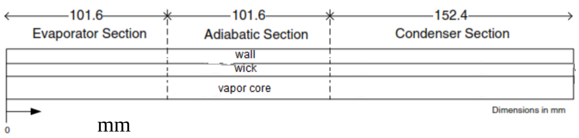

Figure 5: The heat pipe exemple

The physical dimensions of the heat pipe investigated are given in table 2.
We are considering 2D model and the wick is present only on one side of the heat pipe and the heating and cooling boundary conditions are applied only on this wicked side.

Table 2. Physical dimensions of the heat pipe

Description	Dimensions
Heat pipe total length	355.6 *mm*
Evaporator section length	101.6 *mm*
Adiabatic section length	101.6 *mm*
Condenser section length	152.4 *mm*
Heat pipe outer diameter	19.05 *mm*

The wick is made of copper and the working fluid is water. The Thermophysical properties of the heat pipe material and the working fluid are given in table 3.

We are considering two different heat input to the evaporator (Q=60w and Q=140w) while the mean condenser wall temperature was maintained constant (20°C).

Table 3. Thermophysical properties of the heat pipe material and the working fluid

Copper	Thermal conductivity Specific heat Density Wick conductivity	401 *w/m K* 385 *J/kg.K* 8933 kg/m^3 40 *w/m K*
Water liquid	Thermal conductivity Specific heat Density viscosity	0.6 *w/m K* 4200 *J/kg.K* 1000 kg/m^3 8.10^{-4} $N\ s/m^2$
Water vapor	Thermal conductivity Specific heat Density viscosity	0.0189 *w/m K* 1861.54 *J/kg.K* 0.01 kg/m^3 $8.4.10^{-6}$ $N\ s/m^2$
Liquid/vapor	Latent heat	2473 *kJ/kg*

4.2.2. Results

The numerical results of the internal axial temperature distributions in the vapor region are shown in Figure 6 with a constant condenser wall temperature of 20°C and two heat input at the evaporator (Q=60w and Q=140w). As expected, the core temperature in the evaporator increases with heat input power and the temperature in the adiabatic section also increases with heat input power. In the adiabatic zone the vapor receives the heat from the heat pipe wall by axial conduction from the evaporator side. The core temperature in the condenser section is close to that of the condenser wall and it increases with heat input in distance closer to the adiabatic section.

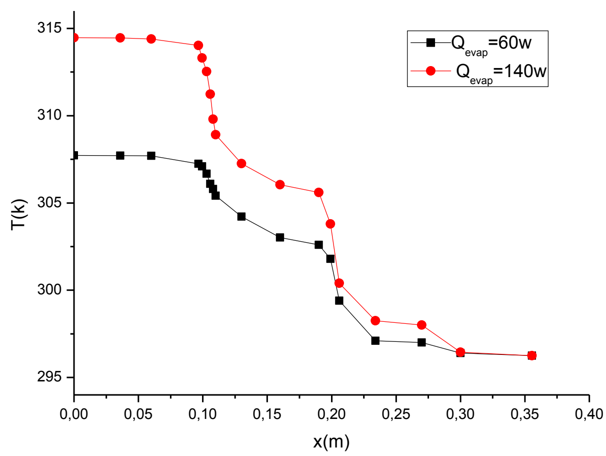

Figure 6: Axial variation of internal core temperature with heat input for a constant condenser wall temperature of 20°C

The Figure 7 shows the numerical result of the wick temperature distribution. We can obviously see the axial temperature variation along heat pipe’s wick. The three sections (evaporator, condenser and adiabatic zone) can be localized and as expected the evaporator and adiabatic wick temperature increases with input power. The evaporator temperature is close to that of the evaporator wall temperature. For the condenser section, the wick temperature increases near the adiabatic section and it decreases to become close to that of the condenser wall.

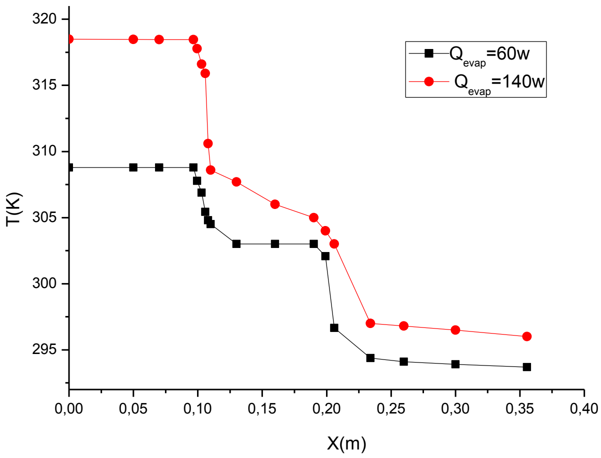

Figure 7: Axial variation of liquid wick temperature with heat input for a constant condenser wall temperature of 20°C

Conclusion

In this work, a new solver is implemented in OpenFOAM to take into account the porous wick region (Darcy term) and the phase change phenomena using VOF model in the object to study heat pipe behavior. We validate this solver with Stefan model in the first step and then with heat pipe model with variation of heat input in the evaporator section. Numerical simulation is compared with the analytical solution of Stefan problem and proves an excellent agreement between them. And in second step, numerical results of the wick and the vapor region temperatures are in line with expected behavior. Future work, we will develop the solver and the phase change phenomena need more work. The effect of various parameters (Operating temperature, heat input, filling rate,…) will be then investigated.

Nomenclature

Symbol	Name, *unity*	Greek Symbols	
p	pressure, *Pa*	ρ	density, kg/m^3
T	Temperature, *K*	ε	porosity of the wick
K	thermal conductivity, *W/m.K*	μ	dynamic viscosity, *kg/m.s*
x	distance, *m*		
Q	heat input, *w*	Exposant, Indices	
c_p	specific heat at constant pressure, *J/kg.K*	v	vapor
A	area, m^2	l	liquid
h_{fg}	latent heat, *J/kg*	i	interface
k	permeability of the wick, m^2	0	reference
m	mass flux, kg/m^2s	Sat	saturation
R	gas constant, *J/kg.K*	eff	effective
t	time, *s*		
U	velocity, *m/s*		
u	longitudinal velocity, *m/s*		
v	transverse velocity, *m/s*		

Références

[1] Frédéric Lefèvre; Conrardy, J ; Raynaud, M ; Bonjour,J, Experimental investigations of flat plate heat pipes with screen meshes or grooves covered with screen meshes as capillary structure, pp. 95-102, 2012.

[2] K.-S. Kim; M.-H. Won; J.-W. Kim; B.-J. Back, Heat pipe cooling technology for desktop PC CPU, Appl. Therm. Eng, 2003.

[3] M. Esen; H. Esen, Experimental investigation of a two-phase closed thermosyphons solar water heater, Sol. Energy, 2005.

[4] M. Esen, Thermal performance of a solar cooker integrated vacuum tube collector with heat pipes containing different refrigerants, Sol. Energy 76, 2004.

[5] M.S. El-Genk; L. Huang, Experimental investigation of the transient response of a water heat pipe, Int. J. Heat Mass Transfer 36 pp. 3823–3830, 1993.

[6] Kempers,R; Robinson, A.J; Ewing, D; Ching, C.Y, Characterization of evaporator and condenser thermal resistances of a screen mesh wicked heat pipe, pp. 6039-6046, 2008.

[7] Martin Andersen, A interphaseChangeFoam tutorial, Chalmers University, 2011.

[8] Vadakkan, Garimella, Murthy, Transport in Flat Heat pipes at High Heat Fluxes from Multiple Discrete Sources, Journal of Heat Transfer, 2004.

[9] CL Merkle and DV Li. Sankaran, Multi-Disciplinary Computational Analysis in Propulsion. AIAA-2006-4374, 42nd AIAA/ASME/SAE/ASEE Joint Propulsion Conference, Sacramento. USA, 2006.

[10] Alexiades, V., Mathematical Modeling of Melting and Freezing Processe.CRC Press, 1992.

[11] Hardt, S., Wondre, F., evaporation model for interfacial flows based on a continuum field representation of the source terms, J. Comput. Phys, 227, 5871-5895, 2008.

[12] Welch, S.W.J., Wilson, J., A volume of fluid based method for fluid flows with phase change, J. Comput. Phys. 160, 662-682, 2000.